Published in final edited form as:
Cell Host Microbe. 2007 July 12; 2(1): 41–53.

Identification of Human MVB12 Proteins as ESCRT-I Subunits that Function in HIV Budding

Eiji Morita[*], **Virginie Sandrin**[*], **Steven L. Alam**[*], **Debra M. Eckert**[*], **Steven P. Gygi**[‖], and **Wesley I. Sundquist**[*,†]

[*]*Department of Biochemistry, University of Utah, Salt Lake City, UT 84112-5650 USA.*

[‖]*Department of Cell Biology, Harvard Medical School, Boston, MA 02115 USA*

SUMMARY

Human ESCRT-I is a multiprotein complex that plays essential roles in HIV budding and endosomal protein sorting. All ESCRT-I complexes contain three common subunits (TSG101, VPS28, and VPS37), and a fourth subunit of yeast ESCRT-I was recently identified (Mvb12p). We now demonstrate that two related human proteins (MVB12A and MVB12B) constitute the fourth class of metazoan ESCRT-I subunits, despite lacking identifiable sequence homology to Mvb12p. Hydrodynamic studies indicate that soluble human ESCRT-I complexes contain one copy of each of the four subunit types. MVB12 subunits associate with the core region of the binary TSG101-VPS37 complex through conserved C-terminal sequence elements. Both MVB12 depletion and overexpression inhibit HIV-1 infectivity and induce unusual viral assembly defects, including aberrant virion morphologies and altered viral Gag protein processing. Taken together, these studies define the composition of human ESCRT-I complexes, and indicate that the MVB12 subunits play a unique role in regulating ESCRT-mediated virus budding.

Keywords

ESCRT-I; HIV budding; MVB12; virus maturation; vacuolar protein sorting

INTRODUCTION

Human ESCRT-I (Endosomal Sorting Complex Required for Transport-I) is a multiprotein complex that helps sort membrane proteins into vesicles that bud into late endosomal compartments called multivesicular bodies (MVB) (Gill et al., 2007b;Gruenberg and Stenmark, 2004;Hurley and Emr, 2006). ESCRT-I also mediates the budding of HIV-1 and other enveloped RNA viruses (Bieniasz, 2006;Demirov and Freed, 2004;Morita and Sundquist, 2004). Hence, ESCRT-I plays essential roles in several significant biological processes, including the release of human pathogens and the essential downregulation of cell surface receptors targeted for lysosomal degradation via MVB vesicles.

Under steady state conditions, ESCRT-I is distributed throughout the cytoplasm, but is transiently recruited to sites of MVB vesicle and virus budding (Katzmann et al., 2001;Martin-Serrano et al., 2001;Welsch et al., 2006). ESCRT-I is recruited to function in HIV-1 budding

[†]Corresponding author: Wesley I. Sundquist, Department of Biochemistry, University of Utah, Salt Lake City, UT 84132-3201, (801) 585-5402 voice, (801) 581-7959 fax, wes@biochem.utah.edu

via direct interactions with the PTAP "late domain" sequence located within the p6 region of the viral Gag polypeptide. Gag is the major viral structural protein and has the intrinsic ability to bind membranes and assemble into spherical particles, but requires the ESCRT-I interaction to accomplish the membrane fission required for efficient virion release. Virion budding initiates viral maturation, a stepwise process that involves: 1) activation of the viral protease, 2) proteolytic cleavage of Gag at a series of different sites to liberate the mature MA, and CA, and NC proteins, and 3) major structural rearrangements involving condensation of the NC-RNA complex and assembly of CA into the conical capsid that surrounds the NC-RNA complex.

In the endosomal pathway, ESCRT-I is recruited to function in MVB vesicle formation through direct interactions with the upstream HRS/Vps27p protein complex (Bache et al., 2003;Katzmann et al., 2003;Lu et al., 2003;Pornillos et al., 2003). Once localized to the membrane, ESCRT-I can bind ubiquitylated protein cargoes and recruit downstream effector complexes such as ESCRT-II and ESCRT-III that help mediate protein sorting and vesicle formation. The assembled ESCRT complexes are then recycled by the action of the VPS4 ATPases, the only known enzymes in the pathway (Babst et al., 1998).

Human and yeast ESCRT-I complexes share at least three homologous subunits, termed TSG101/Vps23p, VPS28/Vps28p and VPS37/Vps37p. Structural and biochemical analyses have revealed that the yeast Vps23p, Vps28p, and Vps37p subunits form a 1:1:1 ternary complex, in which conserved segments from each subunit coassemble into a six helix bundle (Chu et al., 2006;Gill et al., 2007a;Kostelansky et al., 2006;Teo et al., 2006). Each subunit contributes a helical hairpin, which associate side-to-side along their long axes with the Vps23p hairpin in the center. Elsewhere, the ESCRT-I subunits display a series of "effector" domains that interact with other protein binding partners. For example, Vps23p/TSG101 has a predicated coiled-coil element immediately upstream of the core hairpin that has been implicated in protein oligomerization (Chu et al., 2006;Martin-Serrano et al., 2003) and an N-terminal UEV domain that binds both ubiquitin (Garrus et al., 2001;Katzmann et al., 2001;Sundquist et al., 2004;Teo et al., 2004) and proline-rich elements such as the P(S/T)AP elements in HIV-1 $p6^{Gag}$ and HRS/Vps27p (Pornillos et al., 2002).

The basic architecture of mammalian ESCRT-I appears to be similar to that of yeast ESCRT-I because the TSG101/Vps23p, VPS28/Vps28p and VPS37/Vps37p subunits have common domain organizations and related sequences. Mammalian ESCRT-I complexes exhibit greater complexity, however, as mammalian cells express four different, but related VPS37 subunits (termed VPS37A-D) (Bache et al., 2004;Eastman et al., 2005;Stuchell et al., 2004). Each different VPS37 protein contains a region of 150 amino acids that includes the minimal TSG101-binding core element and is related in sequence to yeast Vps37p. The different mammalian VPS37 proteins diverge significantly outside of this conserved region, however, which may allow them to interact with distinct cellular binding partners.

Recently, several groups have characterized a fourth subunit of the yeast ESCRT-I complex, termed Mvb12p (Chu et al., 2006;Curtiss et al., 2007;Gill et al., 2007a;Oestreich et al., 2007). Metazoan homologs of Mvb12p have not yet been identified, although Chu et al. have noted weak sequence similarities between Mvb12p and human apolipoprotein O (Chu et al., 2006). As part of our continuing effort to characterize human ESCRT-I and its role in HIV-1 budding and assembly, we have searched for cellular proteins that bind ESCRT-I. Here, we report the identification and characterization of a fourth class of proteins that function as stable, constitutive subunits of human ESCRT-I and are required for efficient HIV-1 assembly and infectivity.

RESULTS

Identification of MVB12A as a binding partner for the human ESCRT-I complex

The six known human ESCRT-I subunits (One-STrEP-FLAG (OSF)-TSG101, VPS28, and VPS37A-D) were simultaneously co-expressed in 293T cells to create "baits" that could be used to identify ESCRT-I binding proteins. The resulting mixture of ESCRT-I complexes was affinity purified on a Strep-Tactin matrix, which captured TSG101 and stable binding partners. Bound proteins were analyzed by SDS-PAGE (Fig.1A, lane 2), and the ESCRT-I subunits were identified by comparison to known standards. As expected, the tagged TSG101 subunit and the five other overexpressed ESCRT-I subunits were substantially enriched by this procedure. In addition, a seventh endogenous protein with a molecular mass of ~30 KDa reproducibly co-purified with the ESCRT-I complexes (denoted "?" in Fig. 1A, lane 2). This protein was identified by in-gel trypsin digestion and mass spectrometry analyses, which produced 8 different peptides matching those predicted for NCBI protein NP_612410 (273 residues, 41% coverage, see Supplemental Table 1), which is hereafter called MVB12A (Multivesicular Body subunit 12A). Database and literature searches revealed that MVB12A was a previously uncharacterized protein of unknown function and also identified a second related human protein of 319 residues (MVB12B) that shared 30% sequence identity with MVB12A (NCBI protein NP_258257, Supplemental Figure 1).

In addition to MVB12A, a series of other endogenous proteins co-purified with the OSF-TSG101-VPS37-VPS28 complexes, albeit at lower levels. To test whether endogenous MVB12B was one of these co-purifying proteins, a gel section spanning the expected mass of MVB12B (~30-40 KDa) was excised and analyzed by trypsin digestion and mass spectrometry. This experiment confirmed the presence of MVB12B in the affinity purified mixture (4 peptides, 38% coverage, Supplemental Table 1). Hence, both MVB12A and MVB12B proteins were expressed in 293T cells, and both co-affinity purified with overexpressed ESCRT-I complexes, indicating that these two proteins might be ESCRT-I subunits or binding partners.

In related experiments, STrEP-tagged versions of each of the different ESCRT-I proteins were also expressed singly, and trypsin digestion and mass spectrometry were again used to identify other ESCRT-I subunits that co-purified by Strep-Tactin affinity chromatography (Supplemental Table 1). Pairwise interactions between MVB12 proteins and other ESCRT-I subunits were observed 21 different times in these experiments, further confirming that MVB12A and MVB12B associate with the other ESCRT-I subunits in vivo. In contrast, apolipoprotein O, a previously proposed candidate for the mammalian homolog of yeast Mvb12p (Chu et al., 2006), was not detected in any of our proteomics studies.

MVB12A binds all possible human ESCRT-I complexes

To test whether MVB12A could form stable stoichiometric complexes with the other three ESCRT-I subunits, Myc-MVB12A was co-overexpressed together with OSF-TSG101, VPS28, and VPS37B, and complexes were again affinity purified on a Strep-Tactin matrix. As shown in Fig. 1B, equivalent levels of VPS28, VPS37B, and MVB12A co-purified with OSF-TSG101 (lane 2), but did not bind a control matrix (lane 1), indicating that the interactions were specific and were mediated by TSG101. In reciprocal experiments, equivalent levels of Myc-TSG101, VPS28, and Vps37B co-purified with OSF-MVB12A (lane 4), and again did not bind the matrix control (lane 3). Thus, MVB12A forms stable quaternary complexes with TGS101, VPS28 and VPS37B in human cells. Analogous experiments performed for MVB12B showed that TSG101, VPS28, and VPS37B also formed stable complexes with MVB12B (Supplemental Fig. 2A, lanes 2 and 4) without background binding to control matrices (lanes 1 and 3).

We also tested the possibility that specific VPS37 subunits might uniquely pair with specific MVB12 subunits. This was not the case, however, as all four known human VPS37 subunits (VPS37A-D) formed stable quaternary complexes with TSG101-VPS28-MVB12A (Fig. 1C, lanes 1-4) and with TSG101-VPS28-MVB12B (Supplemental Fig. 2B). Thus, human cells express multiple paralogs of both VPS37 and MVB12, and all 8 possible combinations of human ESCRT-I subunits assemble into stable complexes in human cells.

MVB12A binds ESCRT-I through its conserved C-terminus

Deletion analyses were used to map the ESCRT-I binding site(s) on the MVB12 proteins. A summary of the different MVB12 constructs employed in these studies is provided in Supplemental Figure 3. As shown in Fig. 2A, an MVB12A fragment lacking the final 40 residues ($MVB12A_{1-233}$) formed a stable complex with the other three ESCRT-I proteins (lane 3), whereas a construct lacking the final 82 residues ($MVB12A_{1-191}$) did not (lane 4). Conversely, an MVB12A fragment consisting of only the final 82 residues ($MVB12A_{192-273}$) formed a stable ESCRT-I complex (lane 5), demonstrating that the C-terminal region of MVB12A was necessary and sufficient for ESCRT-I binding. The interaction site could not be subdivided further, however, as two non-overlapping C-terminal fragments of MVB12A ($MVB12A_{192-233}$ and $MVB12A_{234-273}$) both bound ESCRT-I (lanes 6 and 7). Hence, MVB12A must contact ESCRT-I through at least two adjacent sites, one located within residues 192-233, and a second within residues 234-273 (termed ESCRT-I Binding Boxes 1 and 2, abbreviated EBB1 and EBB2). An alignment of metazoan MVB12 proteins indicates that the sequence corresponding to MVB12A residues 192-233 (EBB1) is the most highly conserved region of the protein (Supplemental Figure 1), and our mapping experiments indicate that this sequence conservation reflects a conserved ESCRT-I binding function.

MVB12B exhibits additional complexity in that two different splice isoforms of the protein have been identified (NCBI FAM125B, GeneID: #89853). The longer isoform 1 ($MVB12B_{1-319}$) contains both EBB1 and EBB2, whereas the shorter isoform 2 ($MVB12B_{1-221}$) does not. Binding experiments confirmed the expectation that $MVB12B_{1-319}$ bound ESCRT-I, whereas $MVB12B_{1-221}$ did not (Fig. 2A, compare lanes 9 and 10). Furthermore, a fragment of MVB12B corresponding to the EBB1 alone ($MVB12B_{227-271}$) again bound ESCRT-I (Fig. 2A, lane 11), demonstrating that MVB12B EBB1 was also an ESCRT-I binding module. Thus, both MVB12A and MVB12B bind the ESCRT-I complex through conserved C-terminal ESCRT-I Binding Boxes, whereas a shorter MVB12 isoform that is missing this region does not bind ESCRT-I.

MVB12A and MVB12B bind the TSG101-VPS37 binary complex

To map the binding requirements on the ESCRT-I side of the interaction, we first tested whether MVB12A could bind TSG101, VPS37B, or VPS28 alone. As shown in Fig. 2B, Myc-MVB12A did not co-purify at stoichiometric levels with any of the four isolated OSF-tagged ESCRT-I subunits (upper panel, lanes 2-4). We next tested whether MVB12A could bind any of the possible *binary* complexes of other ESCRT-I subunits (lanes 5-10). These experiments revealed that MVB12A bound TSG101-VPS37B subcomplexes (lanes 7 and 8), but none of the other possible ESCRT-I binary complexes (lanes 5, 6, 9, and 10). Control experiments behaved as expected in that MVB12A bound the ternary TSG101-VPS28-VPS37 complex (lane 11), but not the matrix alone (Fig. 2B, lane 1). These experiments imply that a binary TSG101-VPS37 complex is required to create a high affinity MVB12A binding site.

Deletion analyses were performed to map the regions of TSG101 and VPS37B required for MVB12A binding. As shown in Fig. 2C, MVB12A binds the final 159 residues of TSG101 ($TSG101_{231-390}$), which spans the ESCRT-I core (lanes 3 and 8). Similarly, MVB12A binding

mapped to the N-terminal half of VPS37B ($VPS37B_{1-160}$, lanes 6 and 8), which again corresponds to the most conserved region of VPS37 and includes the minimal TSG101 binding site. Thus, MVB12A binds the regions of TSG101 and VPS37 that form the ESCRT-I core (summarized in Fig. 2D).

MVB12 proteins are integral components of native ESCRT-I complexes

Endogenous mammalian ESCRT-I complexes reportedly elute from gel filtration columns with an apparent molecular weight of 300-350 KDa (Babst et al., 2000;Stuchell et al., 2004). This observation is recapitulated in Fig. 3 (panel 1), where anti-TSG101 antibodies were used to follow the gel filtration mobility of native ESCRT-I complexes from crude soluble cell lysates. The apparent molecular weight of human ESCRT-I was estimated to be 270-280 KDa on this calibrated gel filtration column. To test whether endogenous MVB12A is also a constitutive component of ESCRT-I in human cells, anti-MVB12A antibodies were raised and used to track the gel filtration mobility of MVB12A. As shown in panel 2, essentially all of the native MVB12A protein in the extract also precisely co-eluted with TSG101, as well as other ESCRT-I subunits (data not shown). This experiment indicates that endogenous MVB12A is stably associated with ESCRT-I.

Our attempts to perform analogous experiments with MVB12B were unsuccessful because our anti-MVB12B antibodies did not detect the endogenous protein. Nevertheless, the gel filtration experiments shown in Fig. 3 demonstrate that when TSG101, VPS28, and VPS37B were co-overexpressed with either MVB12A (panel 4) or MVB12B (panel 5), the MVB12 proteins again eluted from gel filtration columns in complexes with apparent molecular weights of ~270 KDa. These observations indicate that both MVB12 paralogs quantitatively associate with the other ESCRT-I subunits in cells. Moreover, these exogenous ESCRT-I complexes exhibited the same gel filtration mobilities as native, endogenous ESCRT-I complexes (compare panels 1 and 2 to 4 and 5).

We also tested whether gel filtration mobility could be used to distinguish ESCRT-I complexes that lacked MVB12 subunits by examining the mobility of ESCRT-I complexes from 293T cells in which only TSG101, VPS37B, and VPS28 were highly overexpressed. Although endogenous ESCRT-I subunits were still present in these cells, the endogenous MVB12 subunits were limiting, and the bulk of the tagged TSG101 in the cell was therefore present in TSG101-VPS37B-VPS28 *ternary* complexes. The apparent molecular weight of these ternary complexes (MW_{app}~210 KDa) was lower than that of the quaternary ESCRT-I complexes, as assessed by following the elution of TSG101 (Panel 3) or other ESCRT-I subunits, (data not shown). The shift was modest (MW_{app} ~60 KDa), however, and the TSG101 elution peak was broadened, possibly owing to the presence of both ternary and quaternary complexes, self-association of the ternary complex, or overexpression effects. Importantly, the gel filtration mobility of native ESCRT-I complexes (panels 1 and 2) matched that of the *quaternary* TSG101-VPS37-VPS28/MVB12 complexes (panels 4 and 5) rather than the *ternary* TSG101-VPS37-VPS28 complexes (panel 3). This experiment indicates that most (and perhaps all) endogenous cellular ESCRT-I complexes contain MVB12 subunits, although we cannot rule out the possibility that a minor pool of endogenous ESCRT-I complexes may lack MVB12 subunits owing to the limited resolution of the gel filtration experiment.

Recombinant ESCRT-I complexes bind HIV-1 $p6^{Gag}$ and HRS

As discussed earlier, pure intact recombinant ESCRT-I complexes from higher organisms have not been described previously, both because MVB12 subunits had not been identified and because the proline-rich, N-terminal half of TSG101/Vps23p is difficult to express in *E. coli*. We therefore tested whether the mammalian co-expression system could be used to generate stable, full-length recombinant ESCRT-I complexes for use in biochemical and structural

studies. As shown in Fig. 4A (left panel), milligram quantities of pure recombinant human ESCRT-I could be generated by co-overexpressing all of the subunits in 293T cells, followed by affinity purification on Strep-Tactin agarose, and gel filtration chromatography.

ESCRT-I is recruited to sites of HIV-1 budding by the viral $p6^{Gag}$ protein, and we therefore tested whether this interaction could be recapitulated *in vitro.* As shown in Fig. 4A (middle panel), purified ESCRT-I bound wild type GST-$p6^{Gag}$ protein immobilized on glutathione agarose, as detected in a western blot using anti-FLAG (TSG101) antibodies (lane 2). This interaction appeared to be specific because TSG101/ESCRT-I did not bind to a control GST matrix (lane 1) or to an immobilized GST-$p6^{Gag}$ protein with a point mutation in the key interacting proline residue in the TSG101 binding site ($p6^{Gag}$ P10A, lane 3). In cells, ESCRT-I can be recruited to sites of MVB vesicle formation by the HRS complex. This interaction could also be recapitulated in vitro using pure recombinant ESCRT-I and purified HRS, and the interaction was again specific (Fig. 4A, right panel). Thus, the ESCRT-I interactions with $p6^{Gag}$ and HRS can be recapitulated with pure recombinant proteins.

Soluble, endogenous Human ESCRT-I is a 1:1:1:1 heterotetramer

Several lines of evidence suggest that TSG101 and ESCRT-I have a propensity to self-associate in cells, and it has been proposed that Mvb12p stabilizes a trimeric (or possibly dimeric) form of yeast ESCRT-I (Chu et al., 2006). However, biophysical studies of pure recombinant yeast ESCRT-I complexes indicate that recombinant Vps23p (TSG101), Vps28p, Vps37p and Mvb12p form a stable, 1:1:1:1 complex in solution (Gill et al., 2007a). To date, there have been no reports of the solution mass and stoichiometry of mammalian ESCRT-I complexes.

Equilibrium sedimentation experiments were therefore performed to determine the solution mass of purified ESCRT-I complexes. The predominant form of affinity purified, recombinant ESCRT-I eluted from a gel filtration column with a MW_{app} 280-270 KDa (see Fig. 3). A small amount of recombinant ESCRT-I also eluted as a minor peak of $MW_{app}\sim$ 570 KDa (note that this minor species is not visible in panel 1, and was not detected for endogenous ESCRT-I). Analytical equilibrium sedimentation data for the major recombinant ESCRT-I complex matched that expected for a 1:1:1:1 complex of TSG101:VPS28:VPS37B:MVB12A (Fig. 4B, blue curve), but not for a 2:2:2:2 “dimeric” (red) or higher order complexes. In contrast, the minor ESCRT-I species was successfully modeled as a 2:2:2:2 “dimer” (Supplemental Figure 4). Hence, the major soluble cellular ESCRT-I species contains a single copy of each of the four different subunits. Importantly, the gel filtration mobility of *endogenous* ESCRT-I complexes corresponded well to the mobility of the recombinant 1:1:1:1 ESCRT-I complex (compare panel 1 to panels 4 and 5 in Fig. 3). We therefore conclude that soluble endogenous human ESCRT-I complexes extracted from cells contain single copies of TSG101, VPS37, VPS28, and MVB12.

MVB12A is recruited to Class E compartments as a component of ESCRT-I

Under steady state conditions, ESCRT-I complexes are transiently recruited to endosomal membranes, where they function in MVB vesicle formation and are subsequently released by the action of the VPS4 ATPases (Babst et al., 1997;Babst et al., 1998). Hence, ESCRT-I complexes become trapped on aberrant endosomal compartments (termed Class E compartments) in the presence of dominant negative VPS4 proteins that lack ATPase activity. This system was therefore used to test whether MVB12A was recruited to Class E compartments as a component of ESCRT-I.

As shown in Fig. 5A, epitope tagged wt MVB12A, TSG101, and wt GFP-VPS4A were all distributed throughout the cell when the three wild type proteins were co-overexpressed, together with untagged versions of the other ESCRT-I subunits (upper row). MVB12A also

concentrated on centrosomes (see Supplemental Figure 5). In contrast, all three proteins became concentrated on punctate class E compartments when the overexpressed VPS4A protein lacked ATP binding activity (VPS4A K173Q; middle row). This marked redistribution of MVB12A correlated with the ability of MVB12A to bind ESCRT-I, because a truncated MVB12A protein that lacked the ESCRT-I binding site ($MVB12A_{1-191}$) failed to redistribute to class E compartments (bottom row). These observations were quantified by determining the degree of overlap between the dominant negative VPS4A K173Q protein and the other proteins. As shown in Fig. 5B, most of the wt MVB12A in the cell co-localized with VPS4A K173Q (69 ± 11% colocalization), as did most of the wt TSG101 (70 ± 14% colocalization). In contrast, almost none of the truncated $MVB12A_{1-191}$ protein colocalized with VPS4A K173Q (3.2 ± 1.6%) even though TSG101-VPS4A K173Q colocalization was not significantly affected (60 ± 14%). These experiments indicate that MVB12A is recruited to endosomal membranes through its conserved C-terminal ESCRT-I binding region and is then released from the membrane by the activity of the VPS4 ATPase.

HIV-1 infectivity, but not release, is reduced upon MVB12 depletion

ESCRT-I facilitates HIV-1 budding, and it was therefore of interest to determine whether depletion of MVB12A and MVB12B affects the late stages of HIV-1 replication. As shown in Fig. 6A, we identified two different siRNAs that reduced the endogenous MVB12 protein to nearly undetectable levels (upper panel). Analogous experiments could not be performed for MVB12B, however, owing to our inability to detect the endogenous protein in western blots. Nevertheless, we did identify two different siRNAs that could efficiently deplete exogenously expressed Myc-MVB12B (lower panel). As shown in Fig. 6B, different combinations of the anti-MVB12 siRNA oligonucleotides reduced infectious viral titers 2-5 fold. These experiments indicate that normal cellular levels of MVB12A and MVB12B are required for full HIV-1 infectivity.

Somewhat surprisingly, the phenotypic consequences of MVB12 depletion differed in several respects from depletion of TSG101 (positive control, last lane). Firstly, MVB12 depletion did not reduce viral infectivity to the same extent as TSG101 depletion (42-fold reduction), suggesting that the MVB12 subunits of ESCRT-I may not play as central a role in HIV-1 budding as the TSG101 subunit. Secondly, MVB12 protein depletion did not measurably reduce HIV-1 particle production, as judged by western blotting of particle-associated CA and MA proteins released into culture supernatants (Fig. 6B, middle panel). Thus, the reduction in viral infectivity seen upon depletion of MVB12 proteins was not explained by a proportional reduction in virus budding.

EM analyses were therefore performed to test whether virions released in the absence of MVB12 proteins exhibited an observable morphological defect that might explain their reduced infectivity. As expected, thin-sectioned HIV-1 particles released from wild type cells frequently exhibited conical capsids, which is the hallmark of mature virions. As summarized in Fig. 6C, mature HIV-1 capsids were observed in just over half of the control particles examined (52%). In contrast, depletion of either MVB12A or MVB12B reduced the frequency of mature HIV-1 particles by approximately 2-fold (29% and 27%, respectively) as compared to the wild type control, and instead resulted in the production of an abnormally large number of aberrant particles. These particles were described as “Amorphous” because the virion interiors were highly electron-dense throughout and lacked clearly defined internal structures (see Fig. 6C, lower right panel). Amorphous particles accounted for only about 10% of the virions produced from wild type cells, but much greater percentages of virions produced from MVB12A or MVB12B-depleted cells (29% and 47%, respectively). Hence, the reduced viral infectivity observed upon MVB12 depletion correlated with reduced production of mature virions and increased production of abnormal virions. Although we do not know what causes

the aberrant virion interiors to appear so amorphous, we speculate that additional cellular proteins may be packaged within these particles, thereby increasing their density and obscuring the visualization of normal internal structures. This is suggested in the "gradient" of Amorphous particle morphologies shown in Fig. 6C, where internal core structures appear evident beneath the obscuring density within the lightest particles.

MVB12 overexpression reduces virus release, Gag processing, and viral infectivity

Previous studies have established that overexpression of TSG101 (and TSG101 fragments) dominantly inhibits HIV-1 release and infectivity, presumably by altering the stoichiometry and/or activity of endogenous ESCRT-I complexes (Fig. 7A, compare lanes 1 and 6)(Shehu-Xhilaga et al., 2004). As shown in Fig. 7B, TSG101 overexpression induced a "late domain" phenotype, in which assembling particles frequently remained tethered to the cell through membrane stalks. The interiors of these tethered particles were frequently abnormally dense and amorphous, which was reminiscent of the "Amorphorous" phenotypes observed in virions produced from MVB12-depleted cells. Overexpression of both MVB12A and MVB12B also strongly inhibited HIV-1 infectivity (12- and 15-fold, respectively, Fig. 7A left panel), with parallel reductions in virion release (Fig. 7A, right panel). These reductions in virus release and infectivity were at least partially relieved, however, when the overexpressed MVB12A and MVB12B proteins lacked C-terminal ESCRT-I binding boxes (compare lanes 2 to 3 and lanes 4 to 5), indicating that ESCRT-I binding activity was required for full inhibition.

Once again, the phenotype of the HIV-1 assembly block induced by MVB12 overexpression was unusual in several respects. Firstly, overexpression of MVB12A or MVB12B proteins reduced the levels of intact Gag polyproteins in producer cells only slightly (to 71 ± 8% of control for MVB12A), but dramatically reduced the accumulation of the intracellular MA and CA proteolytic processing products (to 11±3% of control for MVB12A, see Fig. 7A, right middle panel and figure caption). In spite of the strong reduction in particle release caused by MVB12 overexpression, however, the particles that were released had fully processed MA and CA proteins, indicating that Gag was processed in those particles that escaped the cell. EM analyses of the cell-associated viral particles produced in the presence of high levels of MVB12A revealed an additional assembly/budding defect. As shown in Fig. 7B, viral particles produced in cells that overexpressed MVB12A frequently remained cell-associated. Unlike the case of TSG101 overexpression, however, most of these virions were not directly connected to the cell membrane, though they were frequently tethered to one another (and perhaps ultimately to the plasma membrane) through continuous lipid bridges. The tethered virions lacked mature conical capsids, and bore some resemblance to immature viral particles, but with less well delineated Gag shells.

Mutation of MVB12A phosphorylation sites partially relieves the overexpression block

Endogenous MVB12A and MVB12B proteins frequently exhibited multiple banding patterns on SDS-PAGE gels suggestive of protein phosphorylation. Consistent with this observation, multiple threonine and serine phosphorylation sites in both MVB12A and MVB12B were identified by mass spectrometry (Fig. 7C, Supplemental Table 2, and and Supplemental Fig. 6). To begin to test whether MVB12 phosphorylation was functionally important, we created two different expression constructs for mutant MVB12A proteins that lacked phosphorylation sites. The MVB12A 5A construct had alanine mutations in place of the five confirmed MVB12A phosphorylation sites, and the MVB12A 9A construct had four additional mutations that corresponded to mapped phosphorylation sites in MVB12B (Fig. 7C, lower two panels). Both mutant MVB12A proteins expressed well (Fig. 7D, lower right panel) and formed stable ESCRT-I complexes (not shown), indicating that the mutations did not grossly alter MVB12A folding or ESCRT-I association. Nevertheless, the mutations attenuated the ability of overexpressed MVB12A to block HIV-1 infectivity (Fig. 7D, left panel), virion release (upper

right panel), and Gag processing (middle right panel). Thus, MVB12A phosphorylation is not required for ESCRT-I complex formation, but is required for efficient MVB12A-mediated dominant inhibition of HIV-1 release and infectivity. Importantly, this is also the first indication that kinases (and perhaps also phosphatases) are involved in the ESCRT pathway.

DISCUSSION

Our studies reveal that MVB12 proteins are previously unidentified subunits of human ESCRT-I. Closely related MVB12 orthologs are conserved across metazoa, and vertebrates express two distinct, but related MVB12 paralogs (MVB12A and MVB12B). Two other ESCRT-I subunits, TSG101 and VPS28, lack obvious paralogs, whereas mammals express four distinct, but related VPS37 proteins from different genes (VPS37A-D). Soluble ESCRT-I complexes contain single copies of each of the four different subunit types (TSG101, VPS28, VPS37, and MVB12). Hence, the different known VPS37 and MVB12 paralogs can combine to produce up to eight different ESCRT-I variants, and we find that all possible combinations can form stable complexes in cells. Human cells also appear to express: 1) two alternative VPS28 transcripts with different C-termini, one of which has a TSG101-binding PSAP motif (Gill et al., 2007a;Martin-Serrano, 2007), and 2) a truncated splice isoform of MVB12B that lacks ESCRT-I binding activity. Thus, human ESCRT-I is best described as a heterogeneous *family* of related complexes. It is reasonable to expect that the different ESCRT-I isoforms will perform distinct, but possibly overlapping functions. Obvious possible ways in which the different ESCRT-I isoforms could vary include expression patterns, cellular localization, cargo selection, biological functions and/or mechanisms of regulation.

Yeast Mvb12p (12 KDa) is much smaller than both MVB12A (29 KDa) and MVB12B isoform I (36 KDa), and there are no significant regions of sequence similarity. Nevertheless, we believe that the human MVB12 proteins are the functional orthologs of yeast Mvb12p, as both the yeast and human proteins function as stable fourth subunits of ESCRT-I. Moreover, both Mvb12p and MVB12 bind the ESCRT-I core region, although one group has reported that Mvb12p binds the putative leucine zipper region of Vps23p/TSG101 (Chu et al., 2006), whereas another reported that it binds Vps37p (Curtiss et al., 2007). This behavior seems consistent with our observations that: 1) the *binary* TSG101/VPS37 complex forms the minimal binding site for human MVB12 proteins, implying that they may contact both TSG101 and VPS37, and 2) at least two different regions of the MVB12 proteins contact ESCRT-I. Moreover, although the precise functions of both Mvb12p and MVB12 proteins remain to be established, Mvb12p knockouts exhibit attenuated and unusual phenotypes as compared to knockouts of the other yeast ESCRT-I subunits, suggesting that Mvb12p may play a functionally unique or regulatory role in yeast ESCRT-I function (Chu et al., 2006;Curtiss et al., 2007;Oestreich et al., 2007). Similarly, HIV-1 release and infectivity are less severely blocked by MVB12 depletion than by TSG101 depletion, and there are also significant phenotypic differences between the two conditions. Finally, while our manuscript was under review, Hurley and colleagues reported the crystal structure of the heterotetrameric yeast ESCRT-I complex, which revealed a highly elongated complex in which a globular “headpiece” sits at one end of an extended “stalk” (Kostelansky et al., 2007). Our studies are in excellent agreement with their structural and biochemical analyses because they find that yeast ESCRT-I is a 1:1:1:1 complex in which the Mvb12p subunit binds the binary Vps23p/TSG101-Vps37p complex to form the ESCRT-I stalk.

Although our experiments establish that the soluble endogenous ESCRT-I complexes extracted from human cells are 1:1:1:1 complexes of TSG101:VPS28:VPS37:MVB12 (here termed ESCRT-I “monomers”), several important issues still surround ESCRT-I localization and oligomerization within cells. Firstly, self-association of ESCRT-I and its Vps23p/TSG101 subunit has been reported (Chu et al., 2006;Martin-Serrano et al., 2003;von Schwedler et al.,

2003), and we also observed that a small population of stable ESCRT-I dimers formed under overexpression conditions. Secondly, a recent immunolocalization study reported that the majority of ESCRT-I is found in close juxtaposition with cellular membranes (Welsch et al., 2006), whereas all of our analyses were performed on soluble ESCRT-I complexes. We therefore considered the possibility that the Triton detergent used during cell lysis might have altered ESCRT-I oligomerization or membrane association. This was not the case, however, as the soluble endogenous ESCRT-I monomer was also the predominant species when cells were lysed in isotonic saline lacking detergent and the soluble ESCRT-I in these crude lysates was analyzed immediately by gel filtration chromatography (not shown). We therefore conclude that under steady state conditions, human ESCRT-I is a monomer, and any oligomeric or membrane associations must be weak at best. These properties may well change, however, when ESCRT-I is transiently recruited to sites of vesicle formation or virus budding. Indeed, we observe strong endosomal membrane localization of all of the different ESCRT-I subunits, including MVB12A, in the absence of VPS4 ATPase activity, and these membrane-associated multiprotein associations are highly resistant to detergent extraction.

Our data are consistent with the idea that human MVB12 is an important, but not absolutely essential subunit of human ESCRT-I. Importantly, HIV-1 budding and assembly are perturbed when cellular MVB12 levels are altered, indicating that MVB12 functions in HIV-1 release. Specifically, MVB12 protein *depletion* caused moderate (2-5-fold) decreases in viral infectivity, with corresponding increases in the production of electron-dense, amorphous particles. MVB12 protein *overexpression* inhibited HIV-1 release and infectivity even more severely (12-15-fold), and full inhibition required MVB12 proteins that could bind ESCRT-I and be fully phosphorylated. MVB12 overexpression again altered the phenotype of viral assembly, in this case leading to the accumulation of membrane-tethered, immature particles that remained associated with the cell surface. Remarkably, MVB12 overexpression also dramatically reduced the accumulation of intracellular Gag processing intermediates (Fig. 7A, middle right panel, lanes 2 and 4). TSG101 overexpression also alters the processing pattern of cell-associated Gag, but in that case Gag processing is delayed, resulting in an appreciable buildup of the CA-SP1 and p41 processing intermediates (e.g., Fig. 7A, middle right panel, lane 6). Thus, high levels of both MVB12 and TSG101 alter the normal coupling between Gag processing and virus budding, thereby changing the range of cell-associated Gag processing intermediates, but the precise changes in Gag processing are different in the two cases.

Finally, we speculate that MVB12 proteins will also function in the sorting of cellular protein cargoes at the multivesicular body and that they may play a unique role in ESCRT-I function, perhaps in helping to regulate conformational changes, complex release, or other essential ESCRT-I transformations. Evidence in support of a unique regulatory role for MVB12A includes: 1) indications that the yeast homolog, Mvb12p, also regulates various different ESCRT-I activities (Chu et al., 2006;Curtiss et al., 2007;Oestreich et al., 2007), 2) the series of distinctive viral assembly phenotypes that occur in response to altered MVB12 levels, including aberrant virion morphologies and unusual changes in the normal coupling between Gag processing and virus budding, and 3) the extensive number of MVB12A and MVB12B phosphorylation sites, which suggests the possibility of post-translational regulation. More detailed mechanistic studies of ESCRT-I are clearly warranted, and such studies should be facilitated by the identification of MVB12 as the last remaining core subunit of metazoan ESCRT-I and by the development of methods for producing pure recombinant human ESCRT-I complexes.

EXPERIMENTAL PROCEDURES

Cell Cultures

293T cells and HOS-pBABE-puro cells (generously supplied by Dr. Nathan Landau through the AIDS Reference and Reagent Program, cat. #3517) were maintained in DMEM supplemented with 10% FCS. K562 cells were maintained in RPMI-1640 medium supplemented with 10% FCS. To assay HIV-1 production, 5×10^5 293T cells/well (6 well plate) were transfected with 2 μg R9 proviral HIV-1 expression plasmid (Garrus et al., 2001;Swingler et al., 1997). For immunofluorescence experiments, HOS cells were seeded onto coverslips, co-transfected at 50-60% confluence, and imaged as described in the caption to Supplemental Figure 5.

Expression Plasmids

Expression plasmids used in this study are summarized in Supplemental Table 3.

ESCRT-I Complex Purification

For small scale purifications, 293T cells were seeded (3×10^6 cells/55 cm^2 dish) and co-transfected with 3 μg each of ESCRT-I expression plasmids using polyethylenimine (25,000 KDa; Polysciences, Warrington, PA) as described (Durocher et al., 2002). Cells were harvested 48h post-transfection by inclubation in 300 μl lysis buffer (LB: 50mM Tris (pH 7.4), 150mM NaCl) supplemented with proteinase inhibitor cocktail (Sigma) and 1% Triton X-100. Lysates were clarified by centrifugation (18,000 × g, 10 min, 4°) and incubated with Strep-Tactin Sepharose (40 μl slurry, IBA GmbH, Gottingen Germany, 2h, 4°). The matrix was washed 4X in wash buffer (WB: 20 mM Tris (pH 7.4), 150 mM NaCl) supplemented with 0.1% Triton X100, and purified ESCRT-I complexes were eluted with 2.5 mM desthiobiotin in WB. Typical yield: ~30 μg ESCRT-I.

For large scale preparations (e.g., for analytical ultracentrifugation experiments), this basic procedure was scaled up 200-fold, with the following modifications: 1) douncing (100X) was used to promote cell lysis, 2) ESCRT-I complexes were affinity purified on a 5 ml Strep-Tactin Sepharose column (detergent-free LB washes), 3) affinity purified ESCRT-I complexes were concentrated to 2 ml using a Vivaspin 2 concentrator (Vivascience Ltd, 30,000 MW cutoff), and purified by gel filtration in LB (16/26 Superdex 200 column in LB). Recombinant ESCRT-I complexes eluted in two peaks, a major peak (MW_{app} ~280 KDa) and a minor peak (MW_{app} ~570 KDa). This procedure typically yielded 1-2mg purified ESCRT-I (major peak).

Gel Filtration Analyses of ESCRT-I Complexes

K562 or 293T cells expressing endogenous or exogenous ESCRT-I were suspended in PBS ± 0.1% Triton X-100 and proteinase inhibitor cocktail and lysed by douncing. Lysates were clarified by centrifugation (18,000 × g, 10 min, 4°) and chromatographed on a calibrated Superdex 200 gel filtration column. Fractions were collected, and ESCRT-I proteins were detected by western blotting following trichloroacetic acid precipitation and SDS-PAGE.

Equilibrium Sedimentation Analyses

The major and minor ESCRT-I gel filtration peaks were collected separately and concentrated. Equilibrium sedimentation experiments were performed in an Optima XL-I centrifuge (Beckman Coulter) at concentrations of 3.6 and 1.8 μM in 50 mM Tris·HCl (pH 7.5), 150 mM NaCl, 4°C. The major (monomeric) ESCRT-I complex was centrifuged at two speeds (12,000 and 16,000 RPM), and the four resulting data sets were globally fit using Heteroanalysis software (Cole, 2004). Analysis of the ESCRT-I dimer is described in Supplemental Figure 4.

ESCRT-I Binding Assays

Soluble GST and GST-p6^{Gag} fusion proteins were expressed in *E. coli* (Garrus et al., 2001). 50 mL cultures were pelleted, resuspended in 4 ml binding buffer (150 mM NaCl, 1% NP-40, 10% glycerol, 1 mM DTT, 50 mM Tris (pH 8.0)) and lysed by lysozyme treatment (1.2 mg) and sonication (3x). For each binding reaction, protein from 10 μl soluble *E. coli* extract was captured on 15 μl glutathione-Sepharose slurry (Amersham Biosciences). Recombinant HIS-V5-HRS was expressed in Sf21 insect cells following manufacturer's instructions (BaculoDirect™, Invitrogen). Sf21 infected cells were resuspended in LB with 1% Triton X100 and protease inhibitors, and lysed by dounce homogenization. For each binding reaction, protein from 10 ml soluble Sf21 extracts was captured on 15 μl anti-V5 antibody conjugated resin slurry (Sigma). To assess binding, ~0.1 nmol purified recombinant ESCRT-I complex was incubated with ~1.0 nmol of immobilized GST-p6^{Gag}, V5-HRS, or control proteins (1 h, 4°C in WB supplemented with 0.1% Triton X-100). Unbound ESCRT-I was removed by washing with WB, and bound ESCRT-I proteins were released by boiling in SDS-PAGE loading buffer and analyzed by 12% SDS-PAGE with Coomassie staining or western blotting using rabbit anti-FLAG antibody (1:1000, Sigma).

Antibody Production

Antibodies to affinity purified recombinant GST-MVB12A and OSF-MVB12B were raised in New Zealand White Rabbits (Covance, Inc.). MVB12A antibodies were affinity purified by binding to recombinant OSF-MVB12A$_{1-191}$, as described (von Schwedler et al., 2003).

Assays for HIV Release and Infectivity

HIV-1 infections were initiated by transfection of the proviral HIV-1 R9 construct, with cell- and virion-associated Gag proteins detected by western blotting and viral titers measured using single-cycle MAGIC assays as described previously (Garrus et al., 2001). Myc-tagged ESCRT-I proteins were analyzed by western blotting (1:3000 mouse anti-Myc 9E10, Covance).

Electron Microscopy

Procedures for obtaining EM images of free and cell-associated thin-sectioned virions were as described previously (von Schwedler et al., 1998), except that the samples were fixed with 2.5% gluteraldehyde/1%paraformaldehyde and dehydrated with an ethanol series.

Supplementary Material

Refer to Web version on PubMed Central for supplementary material.

ACKNOWLEDGEMENTS

We gratefully acknowledge support from the University of Utah Core Facilities in Electron Microscopy and Fluorescence Imaging and funding from NIH AI051174 (to WIS) and from the American Foundation for AIDS Research (to VS).

REFERENCES

Babst M, Odorizzi G, Estepa EJ, Emr SD. Mammalian tumor susceptibility gene 101 (TSG101) and the yeast homologue, Vps23p, both function in late endosomal trafficking. Traffic 2000;1:248–258. [PubMed: 11208108]

Babst M, Sato TK, Banta LM, Emr SD. Endosomal transport function in yeast requires a novel AAA-type ATPase, Vps4p. EMBO J 1997;16:1820–1831. [PubMed: 9155008]

Babst M, Wendland B, Estepa EJ, Emr SD. The Vps4p AAA ATPase regulates membrane association of a Vps protein complex required for normal endosome function. EMBO J 1998;17:2982–2993. [PubMed: 9606181]

Bache KG, Brech A, Mehlum A, Stenmark H. Hrs regulates multivesicular body formation via ESCRT recruitment to endosomes. J Cell Biol 2003;162:435–442. [PubMed: 12900395]

Bache KG, Slagsvold T, Cabezas A, Rosendal KR, Raiborg C, Stenmark H. The Growth-Regulatory Protein HCRP1/hVps37A is a Subunit of Mammalian ESCRT-I and Mediates Receptor Downregulation. Mol Biol Cell. 2004

Bieniasz PD. Late budding domains and host proteins in enveloped virus release. Virology 2006;344:55–63. [PubMed: 16364736]

Chu T, Sun J, Saksena S, Emr SD. New component of ESCRT-I regulates endosomal sorting complex assembly. J Cell Biol 2006;175:815–823. [PubMed: 17145965]

Cole JL. Analysis of heterogeneous interactions. Methods Enzymol 2004;384:212–232. [PubMed: 15081689]

Curtiss M, Jones C, Babst M. Efficient cargo sorting by ESCRT-I and the subsequent release of ESCRT-I from multivesicular bodies requires the subunit Mvb12. Mol Biol Cell 2007;18:636–645. [PubMed: 17135292]

Demirov DG, Freed EO. Retrovirus budding. Virus Res 2004;106:87–102. [PubMed: 15567490]

Durocher Y, Perret S, Kamen A. High-level and high-throughput recombinant protein production by transient transfection of suspension-growing human 293-EBNA1 cells. Nucleic Acids Res 2002;30:E9. [PubMed: 11788735]

Eastman SW, Martin-Serrano J, Chung W, Zang T, Bieniasz PD. Identification of human VPS37C, a component of endosomal sorting complex required for transport-I important for viral budding. J Biol Chem 2005;280:628–636. [PubMed: 15509564]

Garrus JE, von Schwedler UK, Pornillos OW, Morham SG, Zavitz KH, Wang HE, Wettstein DA, Stray KM, Cote M, Rich RL, et al. Tsg101 and the vacuolar protein sorting pathway are essential for HIV-1 budding. Cell 2001;107:55–65. [PubMed: 11595185]

Gill DJ, Teo H, Sun J, Perisic O, Veprintsev DB, Emr SD, Williams RL. Structural insight into the ESCRT-I/-II link and its role in MVB trafficking. EMBO J 2007a;26:600–612. [PubMed: 17215868]

Gill DJ, Teo H, Sun J, Perisic O, Veprintsev DB, Vallis Y, Emr SD, Williams RL. Structural studies of phosphoinositide 3-kinase-dependent traffic to multivesicular bodies. Biochemical Society symposium 2007b:47–57.

Gruenberg J, Stenmark H. The biogenesis of multivesicular endosomes. Nat Rev Mol Cell Biol 2004;5:317–323. [PubMed: 15071556]

Hurley JH, Emr SD. The ESCRT complexes: structure and mechanism of a membrane-trafficking network. Annu Rev Biophys Biomol Struct 2006;35:277–298. [PubMed: 16689637]

Katzmann DJ, Babst M, Emr SD. Ubiquitin-dependent sorting into the multivesicular body pathway requires the function of a conserved endosomal protein sorting complex, ESCRT-I. Cell 2001;106:145–155. [PubMed: 11511343]

Katzmann DJ, Stefan CJ, Babst M, Emr SD. Vps27 recruits ESCRT machinery to endosomes during MVB sorting. J Cell Biol 2003;162:413–423. [PubMed: 12900393]

Kostelansky MS, Schluter C, Tam YY, Lee S, Ghirlando R, Beach B, Conibear E, Hurley JH. Molecular Architecture and Functional Model of the Complete Yeast ESCRT-I Heterotetramer. Cell 2007;129:485–498. [PubMed: 17442384]

Kostelansky MS, Sun J, Lee S, Kim J, Ghirlando R, Hierro A, Emr SD, Hurley JH. Structural and functional organization of the ESCRT-I trafficking complex. Cell 2006;125:113–126. [PubMed: 16615894]

Lu Q, Hope LW, Brasch M, Reinhard C, Cohen SN. TSG101 interaction with HRS mediates endosomal trafficking and receptor down-regulation. Proc Natl Acad USA 2003;100:7626–7631.

Martin-SerranoJ2007 personal communication and our unpublished results

Martin-Serrano J, Zang T, Bieniasz PD. HIV-1 and Ebola virus encode small peptide motifs that recruit Tsg101 to sites of particle assembly to facilitate egress. Nat Med 2001;7:1313–1319. [PubMed: 11726971]

Martin-Serrano J, Zang T, Bieniasz PD. Role of ESCRT-I in Retroviral Budding. J Virol 2003;77:4794–4804. [PubMed: 12663786]

Morita E, Sundquist WI. Retrovirus budding. Annu Rev Cell Dev Biol 2004;20:395–425. [PubMed: 15473846]

Oestreich AJ, Davies BA, Payne JA, Katzmann DJ. Mvb12 is a novel member of ESCRT-I involved in cargo selection by the multivesicular body pathway. Mol Biol Cell 2007;18:646–657. [PubMed: 17151358]

Pornillos O, Alam SL, Davis DR, Sundquist WI. Structure of the Tsg101 UEV domain in complex with the PTAP motif of the HIV-1 p6 protein. Nat Struct Biol 2002;9:812–817. [PubMed: 12379843]

Pornillos O, Higginson DS, Stray KM, Fisher RD, Garrus JE, Payne M, He GP, Wang HE, Morham SG, Sundquist WI. HIV Gag mimics the Tsg101-recruiting activity of the human Hrs protein. J Cell Biol 2003;162:425–434. [PubMed: 12900394]

Shehu-Xhilaga M, Ablan S, Demirov DG, Chen C, Montelaro RC, Freed EO. Late domain-dependent inhibition of equine infectious anemia virus budding. J Virol 2004;78:724–732. [PubMed: 14694104]

Stuchell MD, Garrus JE, Muller B, Stray KM, Ghaffarian S, McKinnon R, Krausslich HG, Morham SG, Sundquist WI. The Human Endosomal Sorting Complex Required for Transport (ESCRT-I) and Its Role in HIV-1 Budding. J Biol Chem 2004;279:36059–36071. [PubMed: 15218037]

Sundquist WI, Schubert HL, Kelly BN, Hill GC, Holton JM, Hill CP. Ubiquitin recognition by the human TSG101 protein. Mol Cell 2004;13:783–789. [PubMed: 15053872]

Swingler S, Gallay P, Camaur D, Song J, Abo A, Trono D. The Nef protein of human immunodeficiency virus type 1 enhances serine phosphorylation of the viral matrix. J Virol 1997;71:4372–4377. [PubMed: 9151826]

Teo H, Gill DJ, Sun J, Perisic O, Veprintsev DB, Vallis Y, Emr SD, Williams RL. ESCRT-I core and ESCRT-II GLUE domain structures reveal role for GLUE in linking to ESCRT-I and membranes. Cell 2006;125:99–111. [PubMed: 16615893]

Teo H, Veprintsev DB, Williams RL. Structural insights into endosomal sorting complex required for transport (ESCRT-I) recognition of ubiquitinated proteins. J Biol Chem 2004;279:28689–28696. [PubMed: 15044434]

von Schwedler UK, Stemmler TL, Klishko VY, Li S, Albertine KH, Davis DR, Sundquist WI. Proteolytic refolding of the HIV-1 capsid protein amino-terminus facilitates viral core assembly. EMBO J 1998;17:1555–1568. [PubMed: 9501077]

von Schwedler UK, Stuchell M, Muller B, Ward DM, Chung HY, Morita E, Wang HE, Davis T, He GP, Cimbora DM, et al. The protein network of HIV budding. Cell 2003;114:701–713. [PubMed: 14505570]

Welsch S, Habermann A, Jager S, Muller B, Krijnse-Locker J, Krausslich HG. Ultrastructural analysis of ESCRT proteins suggests a role for endosome-associated tubular-vesicular membranes in ESCRT function. Traffic 2006;7:1551–1566. [PubMed: 17014699]

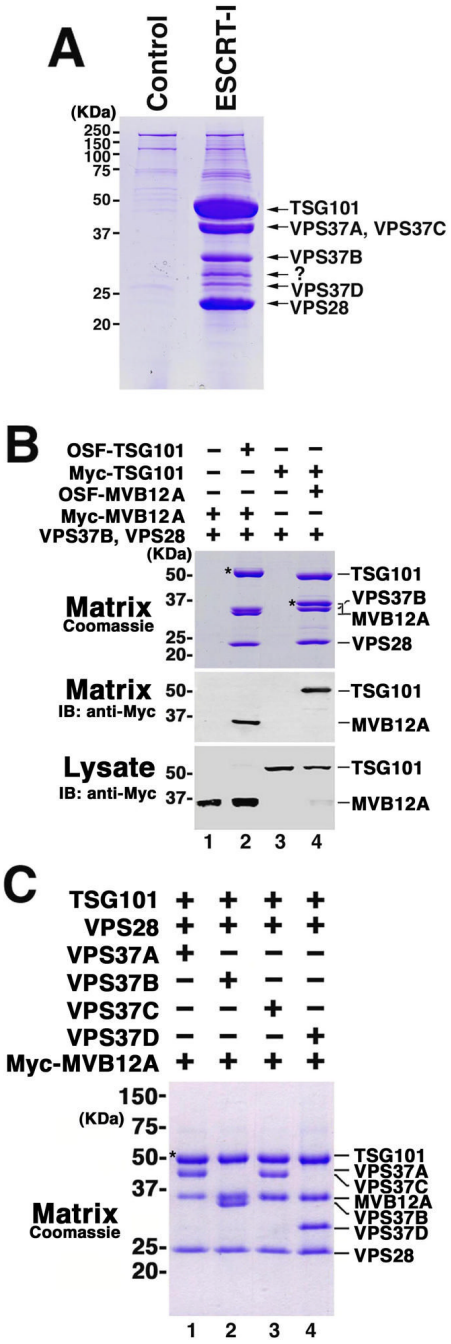

Fig 1. Subunit composition of human ESCRT-I complexes

(**A**) Affinity purification and analysis of Strep-tagged TSG101/ESCRT-I Complexes. All six previously known human ESCRT-I subunits (One-STrEP-FLAG-(OSF)-TSG101, VPS28, VPS37A-D) were simultaneously co-expressed in 293T cells. The resulting complexes were affinity purified on a Strep-Tactin matrix, and visualized by SDS-PAGE (lane 2, Coomassie staining). ESCRT-I subunits co-affinity purifying with OSF-TSG101 are labeled at right, and the band labeled "?" was identified as MVB12A (NCBI: NP_612410). Lane 1 shows background protein binding levels from a control purification from cells transfected with an empty vector.

(**B**) MVB12A forms a stable, stoichiometric complex with TSG101, VPS28, and VPS37B. Lanes 2 and 4 show affinity purification of the quaternary complex when the four proteins were co-expressed with OSF-TSG101 (lane 2) or OSF-MVB12A (lane 4). Asterisks here and throughout denote the tagged “bait” protein. Lanes 1 and 3 show control experiments with extracts that lacked the OSF-tagged subunit. Upper panel: SDS-PAGE gel showing all co-purifying proteins (Coomassie staining). Lower panels: Western blot (anti-Myc) detection of Myc-MVB12A (lanes 1, 2) or Myc-TSG101 (lanes 3, 4) bound to the Strep-Tactin matrix (middle panel) or in the input lysate (lower panel). Note that MVB12A migration changes with the presence or absence of the affinity tag.
(**C**) MVB12A forms stable, stoichiometric ESCRT-I complexes with all four known VPS37 subunits. SDS-PAGE gel (Coomassie staining) showing the proteins that co-affinity purify with OSF-TSG101 from lysates containing overexpressed OSF-TSG101, VPS28, MVB12A, and one of the following: Vps37A (lane 1), Vps37B (lane 2), Vps37C (lane 3), Vps37D (lane 4).

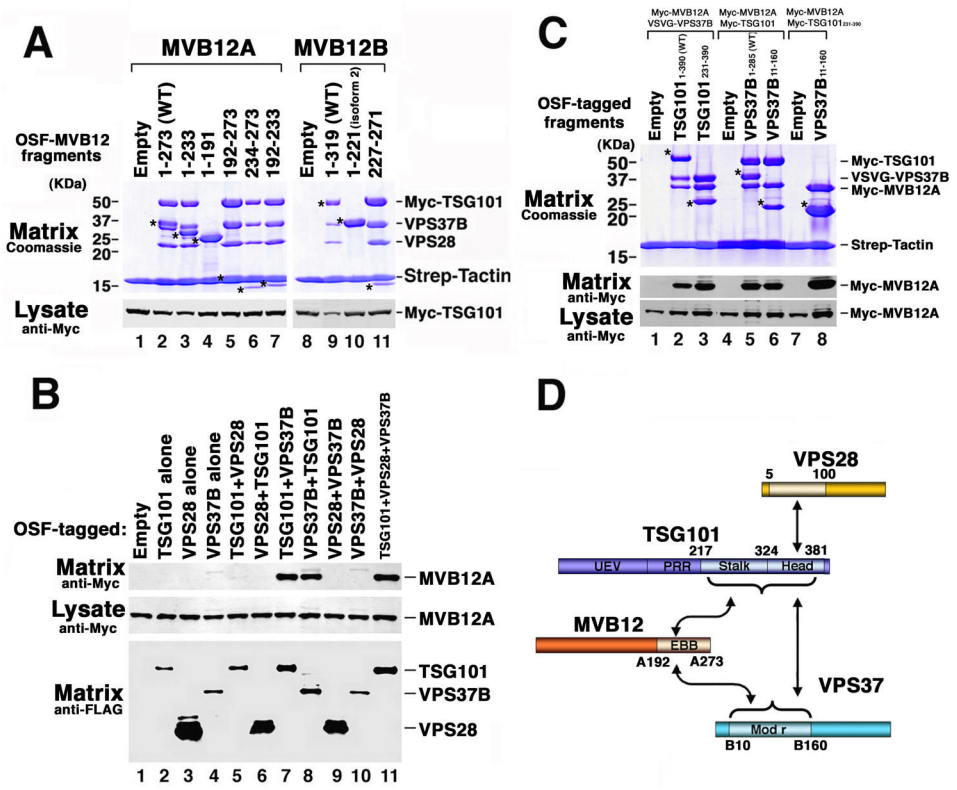

Fig 2. Mapping MVB12-ESCRT-I Interactions

(**A**) Deletion analysis showing the minimal ESCRT-I binding regions on MVB12A and MVB12B. Upper panel shows binding of the TSG101-VPS28-VPS37B ESCRT-I ternary complex to a deletion series of OSF-MVB12A (lanes 2-7) and OSF-MVB12B (Lanes 9-11). Lanes 1 and 8 show background ESCRT-I binding in the absence of the OSF-MVB12 subunit (negative controls). Proteins were visualized by Coomassie staining, and OSF-MVB12 “baits” are designated with asterisks. The lower panel shows a western blot of the input lysates (anti-Myc), confirming the presence of Myc-TSG101.

(**B**) MVB12A binds binary TSG101-VPS37 complexes. Co-purification of Myc-MVB12A with different OSF-tagged and untagged ESCRT-I subunits (indicated above). Upper panel: western blots testing Myc-MVB12A binding to different ESCRT-I subunits and subcomplexes. Lower and middle panels: control western blots confirming expression of MVB12A (middle) and OSF-tagged protein binding to the Strep-Tactin matrix (lower). Controls show lack of Myc-MVB12A binding in the absence of other ESCRT-I subunits (negative control, lane 1), and Myc-MVB12A binding to the TSG101-VPS28-VPS37 ternary complex (positive control, lane 12).

(**C**) Deletion analysis mapping of the minimal MVB12A binding sites on TSG101 and VPS37B. SDS-PAGE gel (Coomassie staining) showing co-purification of full length Myc-MVB12A with different OSF-tagged TSG101 and VPS37B constructs. OSF-tagged baits are given above and are designated by asterisks. Lower panel: Control western blot of the input lysates, confirming the presence of Myc-MVB12A. Middle panel: western blot of the purified complexes (anti-Myc), confirming the presence or absence of Myc-MVB12A.

(**D**) Summary of the ESCRT-I core interaction sites for TSG101, VPS28, VPS37, and MVB12. Core binding regions of TSG101, VPS28, VPS37(A) and MVB12(A) are shown in lighter shades.

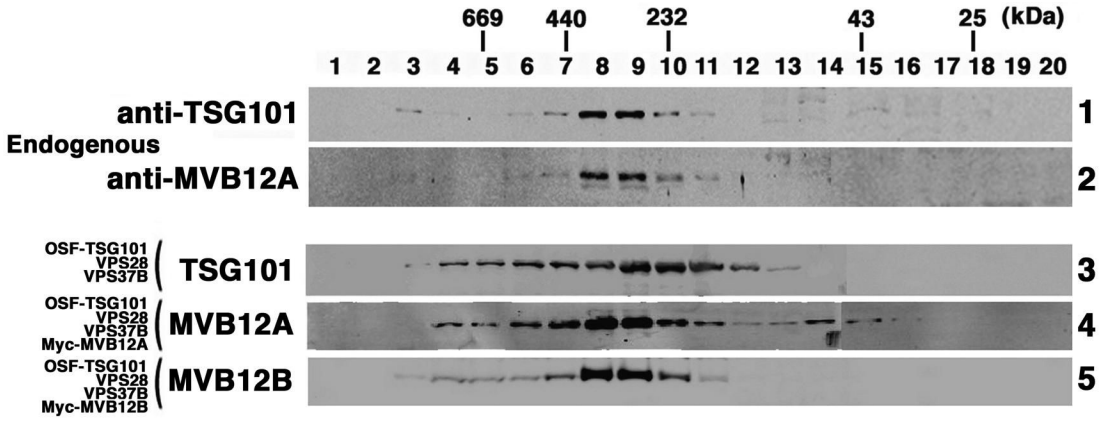

Fig 3. Gel Filtration Chromatography of ESCRT-I Complexes

Panels 1 and 2: Gel filtration mobility and homogeneity of *endogenous* ESCRT-I complexes, as detected by western blotting of crude K562 cell lysates fractionated by gel filtration chromatography and detected with an anti-TSG101 antibody (Panel 1, apparent MW ~270 KDa) or an anti-MVB12A antibody. (Panel 2, apparent MW ~280 KDa). Assayed fractions are given above, together with the positions of molecular weight size markers. Detection with anti-VPS28 and anti-VPS37B antibodies yielded similar results (not shown). Note that breaks between lanes reflect samples run on two different gels.

Panels 3-5: Gel filtration mobilities and homogeneity of *overexpressed* ESCRT-I complexes from 293T cells. Panel 3: Overexpressed OSF-TSG101-VPS28-VPS37B ternary complexes (anti-FLAG detection, MW_{app} ~210 KDa), Panel 4: OSF-TSG101-VPS28-VPS37B-Myc-MVB12A quaternary complexes (anti-Myc detection, MW_{app} ~270). Panel 5: OSF-TSG101-VPS28-VPS37B-Myc-MVB12B quaternary complexes (anti-Myc detection, MW_{app} ~270 KDa).

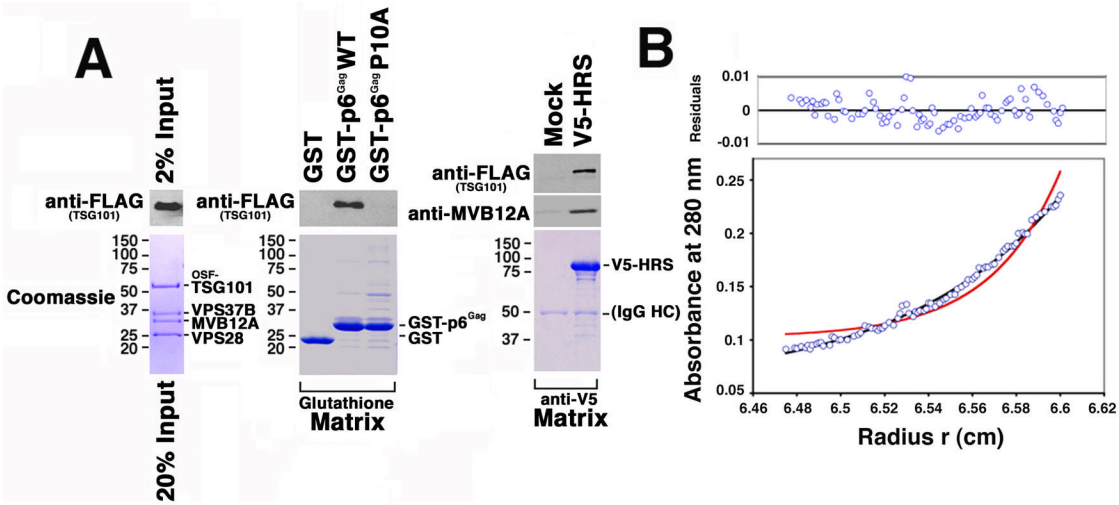

Fig 4. Characterization of Pure Recombinant ESCRT-I Complexes

(**A**) Purified recombinant ESCRT-I binds HIV-1 $p6^{Gag}$ and HRS. Upper Panels: western blots detecting OSF-TSG101 (anti-Flag) or MVB12A (anti-MVB12A). Left Panel: 2% of input ESCRT-I, Central Panel: ESCRT-I binding to GST (negative control), wt HIV-1 $p6^{Gag}$, or HIV-1 $p6^{Gag}$ P10A mutant, Right Panel: ESCRT-I binding to V5-HRS or to a mock purified control. Lower panels: SDS-PAGE (Coomassie staining) showing purified ESCRT-I (left panel, 20% input), GST and GST-$p6^{Gag}$ fusion proteins (middle panel), and V5-HRS (right panel).

(**B**) The solution mass of the major complex of purified recombinant human ESCRT-I corresponds to a monomeric 1:1:1:1 complex of OSF-TSG101:VPS27:VPS28:MVB12A. The equilibrium sedimentation distribution of purified ESCRT-I complexes is shown (16,000 rpm, 3.6 μM ESCRT-I, 4°C). The black line shows the global fit of an ideal single species model to centrifugation data from two speeds and two protein concentrations (MW_{est}=130 KDa, $MW_{monomer}$=134 KDa). For comparison, the distribution expected for a 2:2:2:2 dimeric ESCRT-I complex is shown in red.

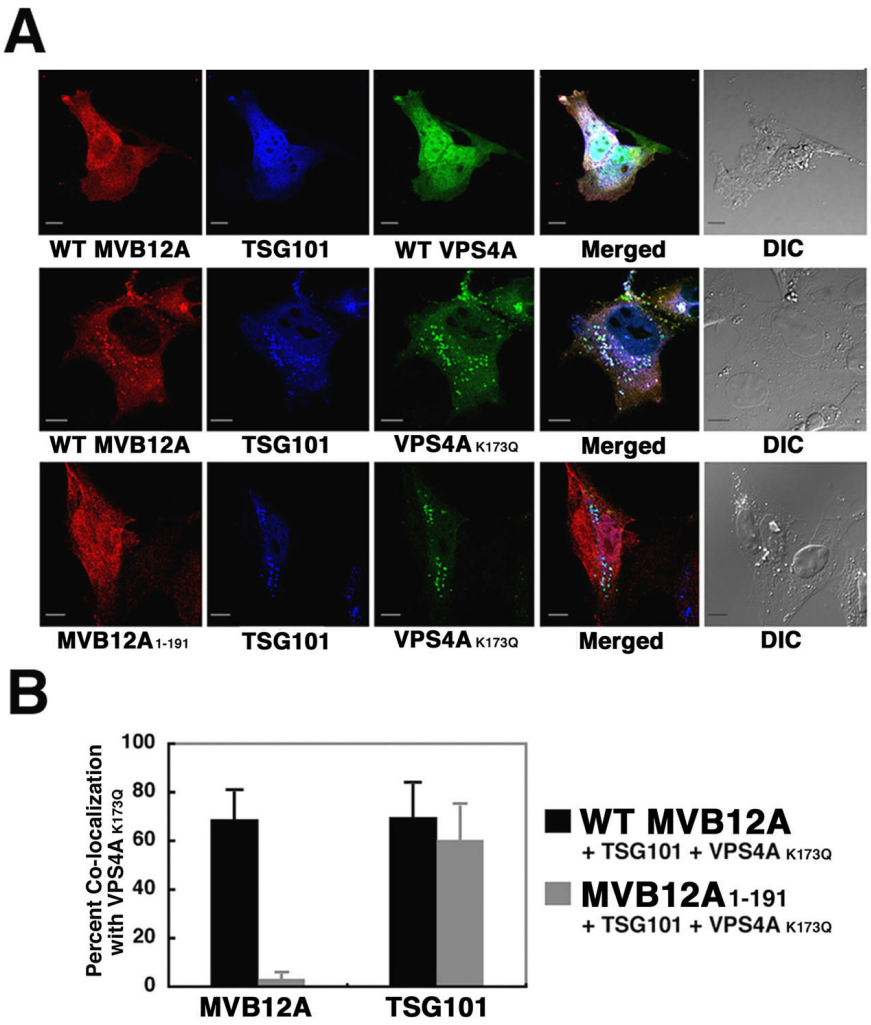

Fig 5. Mutant VPS4 Proteins Relocalize TSG101 and MVB12A to Class E MVB Compartments

(**A**) Confocal immunofluorescence z-slices showing co-localization of different OSF-MVB12A (red), Myc-TSG101 (blue) and VPS4A-GFP (green) proteins (note that untagged VPS28 and VPS37B were also co-overexpressed). Top Row: Co-localization of the wild type proteins, Middle Row: Co-localization with a VPS4A ATPase binding mutant ($VPS4_{K173Q}$), Lower Row: Co-localization with $VPS4A_{K173Q}$, and a truncated MVB12A protein ($MVB12A_{1-191}$) that lacked the ESCRT-I binding site. Merged images are shown in column 4, with white indicating full co-localization, and DIC images are shown in column 5. Scale bars represent 10 μM

(**B**) Quantification of the percentage co-localization of $VPS4A_{K173Q}$ with MVB12A or TSG101 in the presence of WT MVB12A or $MVB12A_{1-191}$ (n= 20 cells/data point).

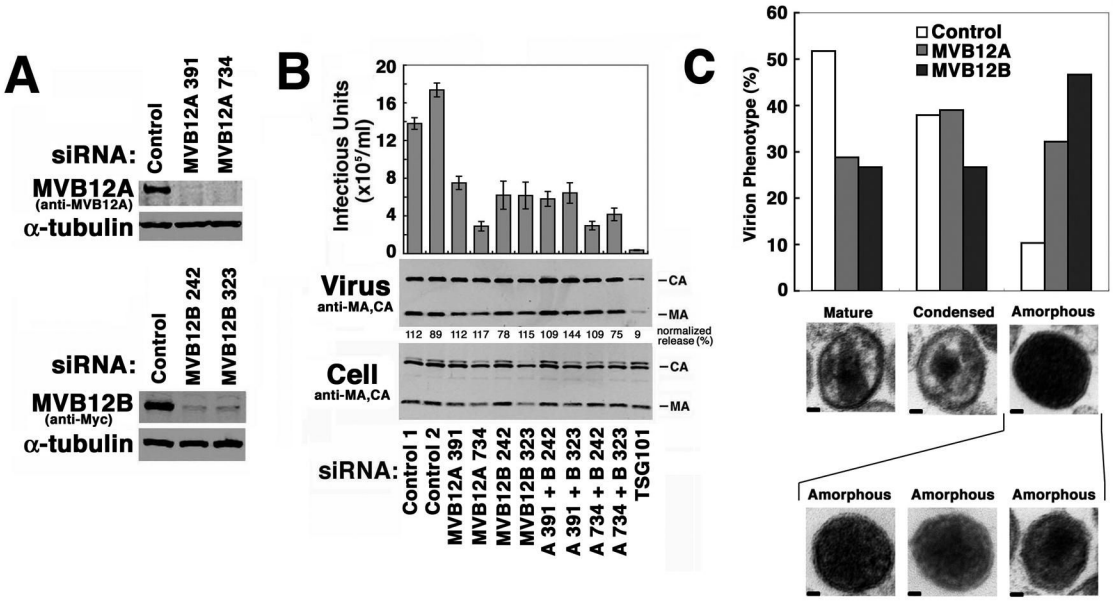

Fig 6. siRNA Depletion of MVB12 Proteins Inhibits HIV-1 Infectivity and Viral Maturation

(**A**) siRNA depletion of endogenous MVB12A (upper panel) and overexpressed MVB12B (lower panel). siRNA names denote the first nucleotide targeted by the 21 nt (19 nt + TT overhang) siRNA duplexes.

(**B**) Upper panel: reduction in HIV-1 infectivity upon depletion of MVB12 proteins. Middle panel: viral particle release as analyzed by western blotting. Lower panel: cellular MA and CA expression levels.

(**C**) EM analysis and quantification of viral maturation phenotypes from control cells (white bars) or from cells depleted of MVB12A (grey) or MVB12B (black). EM images show representative examples of Mature and Condensed phenotypes, together with a continuum of Amorphous phenotypes. Percentages were derived by scoring >40 randomly selected virions released under each condition. Note that “Condensed” phenotypes may simply arise when mature conical cores are imaged in cross section. Scale bars are 10 nm.

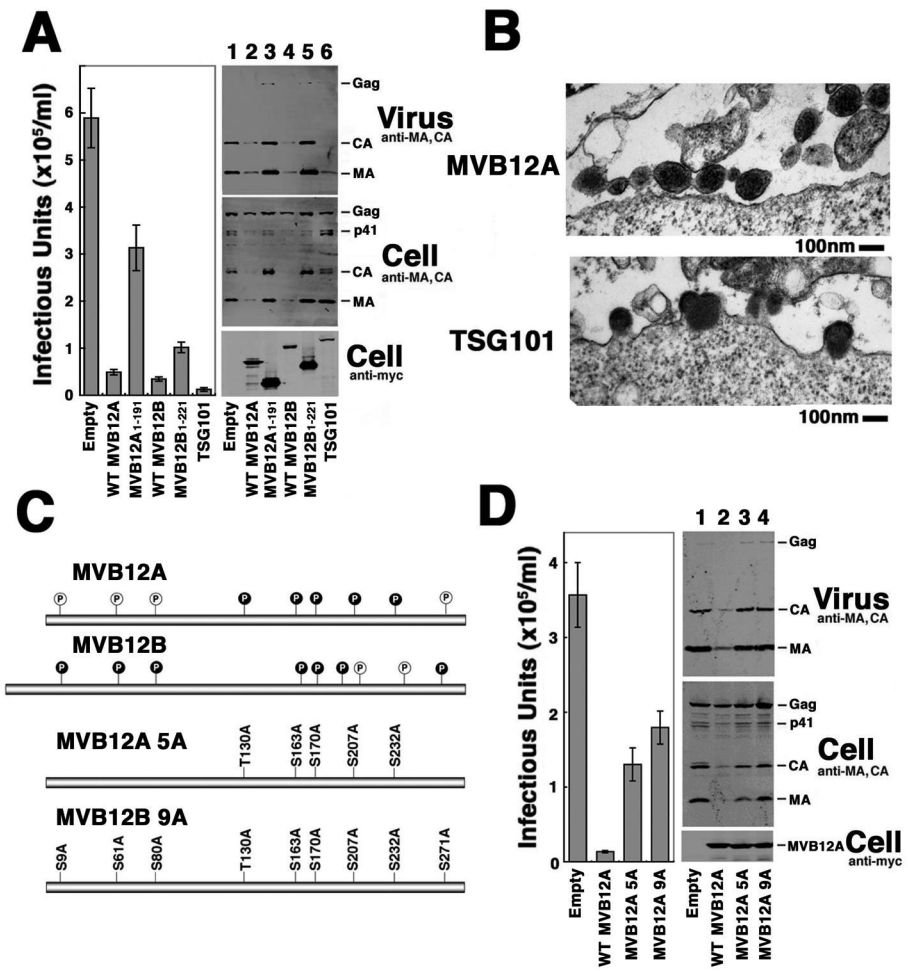

Fig 7. MVB12 Overexpression Inhibits HIV-1 Release, Infectivity, and Processing

(**A**) Reductions in HIV-1 release and infectivity upon overexpression of MVB12A or MVB12B. Left panel shows infectivity data. Upper right panel is a western blot showing levels of HIV-1 particles released into the supernatant (anti-MA and anti-CA detection). Middle right panel shows cellular expression levels and proteolytic processing of Gag (anti-MA and anti-CA detection). Lower right panel shows cellular MVB12 expression levels (anti-Myc). Western blotting data from lane 2 in this figure and in Fig. 7D were quantified to determine changes in protein levels upon MVB12A overexpression (relative to control conditions, lanes 1): Cell-associated Gag protein, 71±8%; Cell-associated CA+MA proteins, 11±3%; Virion-associated CA+MA proteins, 16±5%.

(**B**) EM analyses showing aberrant particles released from 293T cells depleted of MVB12A (upper panel) or TSG101 lower panel.

(**C**) Summary of the mapped (black) or putative (white) phosphorylation sites on MVB12A and MVB12B (upper two panels) and MVB12A 5A and 9A mutant constructs (lower two panels).

(**D**) MVB12A phosphorylation mutations abrogate dominant inhibition of HIV-1 release and infectivity. Left panel shows infectivity data. Upper right panel is a western blot showing levels of HIV-1 particles released into the supernatant (anti-MA and anti-CA detection). Middle right panel shows cellular expression levels and proteolytic processing of Gag (anti-MA and anti-CA detection). Lower right panel shows cellular MVB12A expression levels (anti-Myc).